

Extension of the CIPSI-Driven CC($P;Q$) Approach to Excited Electronic States

Swati S. Priyadarsini^a, Karthik Gururangan^a, Piotr Piecuch^{a,b,*}

^aDepartment of Chemistry, Michigan State University, East Lansing, Michigan 48824, USA

^bDepartment of Physics and Astronomy, Michigan State University, East Lansing, Michigan 48824, USA

Abstract

We extend the CIPSI-driven CC($P;Q$) methodology [K. Gururangan *et al.*, J. Chem. Phys. 155 (2021) 174114], in which the leading higher-than-doubly excited determinants are identified using the selected configuration interaction (CI) approach abbreviated as CIPSI, to excited electronic states via the equation-of-motion (EOM) coupled-cluster (CC) formalism. By examining vertical excitations in CH⁺ at equilibrium and stretched geometries, adiabatic excitations in CH, and ground- and excited-state potential cuts of water, we demonstrate that the CIPSI-driven CC($P;Q$) method converges parent CC/EOMCC singles, doubles, and triples energetics from relatively inexpensive Hamiltonian diagonalizations in CI spaces smaller than the corresponding triples manifolds.

Keywords: Coupled-Cluster Theory, Equation-of-Motion Coupled-Cluster Formalism, Excited Electronic States, CIPSI-Driven CC($P;Q$) Approach, Electronic Excitations in CH⁺ and CH, Excited-State Potentials of Water

1. Introduction

An accurate determination of excited electronic states, which lie at the heart of spectroscopy and photochemistry, remains one of the biggest challenges of contemporary quantum chemistry, especially when excited states dominated by two- or other many-electron transitions and excited-state potential energy surfaces (PESs) along bond-stretching coordinates are examined. Meeting this challenge requires the development of reliable, yet practical, methods that can deliver high-quality and well-balanced results for excitation as well as total ground- and excited-state energies at manageable computational costs. In this work, we focus on a promising new approach that can achieve these objectives within the equation-of-motion (EOM) extension [1] of single-reference coupled-cluster (CC) theory [2, 3].

In the EOMCC formalism and its closely related linear-response (LR) [4] CC and symmetry-adapted-cluster configuration interaction (CI) [5] counterparts, the excited-state wave functions of an N -electron system are expressed as $|\Psi_\mu\rangle = R_\mu|\Psi_0\rangle = R_\mu e^T |\Phi\rangle$, where $|\Phi\rangle$ is the reference determinant defining the Fermi vacuum and $T = \sum_{n=1}^N T_n$ and $R_\mu = \sum_{n=0}^N R_{\mu,n} = r_{\mu,0}\mathbf{1} + \sum_{n=1}^N R_{\mu,n}$ are the cluster and EOM excitation operators, respectively, with T_n and $R_{\mu,n}$ representing their n -body components and $\mathbf{1}$ denoting the unit operator. The basic EOMCC approach with singles and doubles (EOMCCSD) [1], which is obtained by truncating T and R_μ at their two-body components and characterized by relatively inexpensive computational steps that scale with the system size \mathcal{N} as $\mathcal{O}(\mathcal{N}^6)$, is useful in describing excited states dominated by one-electron transitions, but it fails in more multireference (MR) situations, such as excited-state potentials along bond-stretching coordinates and excited states with substantial double-excitation character [6–10] (EOMCCSD may struggle with singly excited states too [10]). A conceptually straightforward remedy to most of the problems encountered in EOMCCSD computations is the next method in the EOMCC hierarchy, namely, the EOMCC approach with a full treatment of singles, doubles, and triples (EOMCCSDT) [6, 7, 11], in which T and R_μ are truncated at T_3 and $R_{\mu,3}$, respectively, but the improvements in the EOMCCSD results offered by EOMCCSDT come at a very high price, as the iterative steps characterizing EOMCCSDT calculations scale as $\mathcal{O}(\mathcal{N}^8)$, rendering them prohibitively expensive for all but very small molecules. It is, therefore, desirable to develop approximations to full EOMCCSDT capable of recovering EOMCCSDT energetics at small fractions of the computational effort. Over

*Corresponding author

Email address: piecuch@chemistry.msu.edu (Piotr Piecuch)

the years, a variety of EOMCC and LRCC schemes have been proposed that use arguments originating from many-body perturbation theory (MBPT) to correct EOMCCSD or LRCCSD excitation energies for the leading T_3 and $R_{\mu,3}$ correlations in an iterative or noniterative fashion [12–15], but the resulting approaches, while accurate for excited states dominated by one-electron transitions, are generally insufficient for states with larger contributions from doubly excited configurations and for excited-state potentials along bond-stretching coordinates. The more robust completely renormalized (CR) triples corrections to EOMCCSD [8, 10, 16–19], such as CR-EOMCC(2,3) [17, 18, 20] and its size-intensive δ -CR-EOMCC(2,3) [10, 19] extension, their analogs based on partitioning the similarity-transformed Hamiltonian [21, 22], and the active-space EOMCCSDt approach [6, 7], can handle doubly excited states and excited-state potentials, but they fail to accurately approximate the parent EOMCCSDT energetics when the coupling between the T_n and $R_{\mu,n}$ amplitudes with $n \leq 2$ and their higher-rank T_3 and $R_{\mu,3}$ counterparts becomes large [8, 9, 23].

As shown in Refs. [9, 23], problems encountered in calculations using perturbative, CR-type, and active-space approximations to EOMCCSDT can be alleviated by adopting the CC($P;Q$) framework introduced in Ref. [20]. The CC($P;Q$) formalism, which applies to ground [20, 24–34] and excited [9, 20, 23] states, generalizes the biorthogonal moment expansions that led to the aforementioned CR-EOMCC(2,3) and δ -CR-EOMCC(2,3) approaches and their ground-state CR-CC(2,3) counterpart [35], to unconventional truncations in the T and R_μ operators. By incorporating the leading contributions to the T_n and $R_{\mu,n}$ components with $n > 2$ into the CC/EOMCC iterations, *i.e.*, by relaxing the lower-rank T_1 , T_2 , $R_{\mu,1}$, and $R_{\mu,2}$ amplitudes in the presence of their higher-rank counterparts, and capturing the remaining correlations of interest using suitably defined energy corrections, CC($P;Q$) calculations can accurately approximate high-level CC/EOMCC energetics, such as those of CCSDT [36, 37] and EOMCCSDT, with substantially reduced computational costs, even when T_3 and $R_{\mu,3}$ amplitudes and MR effects become larger [9, 20, 23–34]. The CC($P;Q$) approaches targeting CCSDT developed to date include the active-orbital-based CC(t;3) method [20, 24–28] and its more black-box semi-stochastic [23, 29, 30, 32], adaptive [33], and selected-CI-driven [31, 34] counterparts. The semi-stochastic, adaptive, and active-orbital-based CC($P;Q$) methods targeting EOMCCSDT have been implemented too [9, 23], but the analogous excited-state extension of the CC($P;Q$) approach using the selected CI algorithm abbreviated as CIPSI [38–40], which showed considerable promise in ground-state applications [31, 34], has not yet been developed. We address this gap in the present work. To test the efficiency of the excited-state CIPSI-driven CC($P;Q$) method, which uses relatively small Hamiltonian diagonalizations to identify the dominant triply excited determinants for inclusion in the iterative steps of the CC($P;Q$) procedure, in converging EOMCCSDT energetics, we apply it to vertical excitations in the equilibrium and stretched CH⁺ ion, adiabatic excitations in the CH radical, and ground- and 11 excited-state PES cuts of the water molecule along the O–H bond breaking coordinate.

2. Theory

The CC($P;Q$) calculations for ground and excited electronic states employ a two-step workflow. In the first step – abbreviated as CC(P) for the ground ($\mu = 0$) state and EOMCC(P) for excited ($\mu > 0$) states – we solve the CC/EOMCC equations in a subspace of the N -electron Hilbert space, designated as $\mathcal{H}^{(P)}$ and referred to as the P space, which consists of the excited determinants $|\Phi_K\rangle = E_K|\Phi\rangle$ that, together with the reference determinant $|\Phi\rangle$, dominate the ground- and excited-state wave functions $|\Psi_\mu\rangle$ of interest (E_K denotes an elementary particle–hole excitation operator generating $|\Phi_K\rangle$ from $|\Phi\rangle$). Thus, we start by solving for the amplitudes t_K that define the P -space cluster operator

$$T^{(P)} = \sum_{|\Phi_K\rangle \in \mathcal{H}^{(P)}} t_K E_K \quad (1)$$

associated with the CC(P) ground state $|\Psi_0^{(P)}\rangle = e^{T^{(P)}}|\Phi\rangle$ and energy $E_0^{(P)} = \langle\Phi|\bar{H}^{(P)}|\Phi\rangle$, where $\bar{H}^{(P)} = e^{-T^{(P)}}He^{T^{(P)}}$ is the similarity-transformed Hamiltonian, and diagonalizing $\bar{H}^{(P)}$ in the P space to determine the EOMCC(P) excited-state energies $E_\mu^{(P)}$ and the corresponding particle–hole and hole–particle excitation and deexcitation operators,

$$R_\mu^{(P)} = r_{\mu,0}\mathbf{1} + \sum_{|\Phi_K\rangle \in \mathcal{H}^{(P)}} r_{\mu,K} E_K \quad (2)$$

and

$$L_\mu^{(P)} = \delta_{\mu,0}\mathbf{1} + \sum_{|\Phi_K\rangle \in \mathcal{H}^{(P)}} l_{\mu,K}(E_K)^\dagger, \quad (3)$$

respectively, where the $r_{\mu,K}$ and $l_{\mu,K}$ coefficients define the EOMCC(P) ket states $|\Psi_{\mu}^{(P)}\rangle = R_{\mu}^{(P)} e^{T^{(P)}} |\Phi\rangle$ and the CC(P) ($\mu = 0$) or EOMCC(P) ($\mu > 0$) bra states $\langle \tilde{\Psi}_{\mu}^{(P)} | = \langle \Phi | L_{\mu}^{(P)} e^{-T^{(P)}}$ satisfying the biorthonormality condition $\langle \tilde{\Psi}_{\mu}^{(P)} | \Psi_{\nu}^{(P)} \rangle = \delta_{\mu,\nu}$ ($\delta_{\mu,\nu}$ is the usual Kronecker delta). Once $T^{(P)}$, $L_0^{(P)}$, and $E_0^{(P)}$ and, in the case of excited states, $R_{\mu}^{(P)}$, $L_{\mu}^{(P)}$, and $E_{\mu}^{(P)}$ ($\mu > 0$) are obtained, we proceed to the second step of the CC($P;Q$) procedure, in which the CC(P) and EOMCC(P) energies $E_{\mu}^{(P)}$ are corrected for the remaining correlation effects using the state-specific noniterative corrections

$$\delta_{\mu}(P;Q) = \sum_{|\Phi_K\rangle \in \mathcal{H}^{(Q)}} \ell_{\mu,K}(P) \mathfrak{M}_{\mu,K}(P), \quad (4)$$

calculated with the help of another subspace of the N -electron Hilbert space, referred to as the Q space, denoted as $\mathcal{H}^{(Q)}$ [$\mathcal{H}^{(Q)} \subseteq (\mathcal{H}^{(0)} \oplus \mathcal{H}^{(P)})^{\perp}$, where $\mathcal{H}^{(0)} = \text{span}\{|\Phi\rangle\}$]. The quantities $\mathfrak{M}_{\mu,K}(P)$ entering Eq. (4), defined as $\mathfrak{M}_{0,K}(P) = \langle \Phi_K | \bar{H}^{(P)} | \Phi \rangle$ for the ground state and $\mathfrak{M}_{\mu,K}(P) = \langle \Phi_K | \bar{H}^{(P)} R_{\mu}^{(P)} | \Phi \rangle$ for excited states, are the generalized moments of the CC(P) ($\mu = 0$) and EOMCC(P) ($\mu > 0$) equations representing projections of these equations on the Q -space determinants $|\Phi_K\rangle \in \mathcal{H}^{(Q)}$. The coefficients $\ell_{\mu,K}(P)$ that multiply moments $\mathfrak{M}_{\mu,K}(P)$ in Eq. (4) are calculated as $\ell_{\mu,K}(P) = \langle \Phi | L_{\mu}^{(P)} \bar{H}^{(P)} | \Phi_K \rangle / D_{\mu,K}^{(P)}$, where $D_{\mu,K}^{(P)} = E_{\mu}^{(P)} - \langle \Phi_K | \bar{H}^{(P)} | \Phi_K \rangle$ is the Epstein–Nesbet-style denominator. The final CC($P;Q$) energies are determined using the formula

$$E_{\mu}^{(P+Q)} = E_{\mu}^{(P)} + \delta_{\mu}(P;Q). \quad (5)$$

All that is needed now is a reliable procedure for designing the P and Q spaces that would allow us to accurately and efficiently capture the many-electron correlation effects characterizing the ground and excited states of interest. In this study, where our objective is to accurately approximate CCSDT/EOMCCSDT energetics by extending the CIPSI-driven CC($P;Q$) methodology of Refs. [31, 34] to excited states, the P spaces used in the iterative CC(P) and EOMCC(P) steps are spanned by all singly and doubly excited determinants and the leading triply excited determinants identified with the help of the CIPSI algorithm. The complementary Q spaces, needed to evaluate the CC($P;Q$) corrections $\delta_{\mu}(P;Q)$, are defined as the remaining triply excited determinants not captured by CIPSI, such that the union of the P and Q spaces always consists of all singly, doubly, and triply excited determinants.

We recall that the CIPSI method, proposed in Ref. [38] and subsequently developed in Refs. [39, 40], constructs an approximation to full CI through a sequence of Hamiltonian diagonalizations in increasingly large, iteratively defined, subspaces of the many-electron Hilbert space, denoted as $\mathcal{V}_{\text{int}}^{(k)}$, where $k = 0, 1, 2, \dots$ enumerates consecutive CIPSI iterations. After defining the initial subspace $\mathcal{V}_{\text{int}}^{(0)}$, which in the calculations carried out in this study consisted of the restricted Hartree–Fock (RHF) or restricted open-shell Hartree–Fock (ROHF) determinant for the ground state and the leading configuration-state functions (CSFs) for the lowest-energy states belonging to irreducible representations (irreps) other than that of the ground state, each subsequent subspace $\mathcal{V}_{\text{int}}^{(k+1)}$ with $k \geq 0$ is obtained by augmenting its $\mathcal{V}_{\text{int}}^{(k)}$ predecessor with a subset of the leading singly and doubly excited determinants generated from it identified with the help of MRMBPT, adding them, one by one, to $\mathcal{V}_{\text{int}}^{(k)}$ until the dimension of $\mathcal{V}_{\text{int}}^{(k+1)}$ exceeds that of $\mathcal{V}_{\text{int}}^{(k)}$ by a user-defined factor $f > 1$ (the number of determinants in $\mathcal{V}_{\text{int}}^{(k+1)}$ is usually somewhat larger than f times the dimension of $\mathcal{V}_{\text{int}}^{(k)}$, since additional determinants may have to be incorporated in $\mathcal{V}_{\text{int}}^{(k+1)}$ to ensure that the resulting wave functions are eigenfunctions of the total spin operators S^2 and S_z). The CIPSI diagonalization sequence is terminated either when the second-order MRMBPT corrections, used to correct the raw CIPSI energies obtained in Hamiltonian diagonalizations, fall below a user-specified threshold η , or when the number of determinants in $\mathcal{V}_{\text{int}}^{(k+1)}$ exceeds an input parameter $N_{\text{det(in)}}$. In this work, where we examine the convergence of the CIPSI-driven CC($P;Q$) energies toward CCSDT/EOMCCSDT as a function of $N_{\text{det(in)}}$, we follow Refs. [31, 34] and adopt the latter termination criterion. We stop when the number of determinants in the final wave function $|\Psi^{(\text{CIPSI})}\rangle$, $N_{\text{det(out)}}$, of a CIPSI run providing the list of triply excited determinants for inclusion in the P space satisfies $N_{\text{det(out)}} \geq N_{\text{det(in)}}$.

With the above information in mind, the key steps of the CIPSI-based CC($P;Q$) algorithm for ground and excited states developed in this work, designed to recover the CCSDT/EOMCCSDT-quality energetics, are as follows:

1. Choose a wave function termination parameter $N_{\text{det(in)}}$ and run a CIPSI calculation starting from a suitably chosen zeroth-order subspace $\mathcal{V}_{\text{int}}^{(0)}$ (spanned by the RHF or ROHF determinant) to obtain the ground $|\Psi^{(\text{CIPSI})}\rangle$ state. If there is interest in electronic states belonging to irreps other than that of the ground state, execute the analogous CIPSI runs for lowest-energy states of these other irreps as well.

2. Extract a list or, if states belonging to multiple irreps are targeted, lists of triply excited determinants from the $|\Psi^{(\text{CIPSI})}\rangle$ wave function(s) obtained in Step 1 to determine the P space(s) for the CC(P) and EOMCC(P) calculations. For the ground state and excited states belonging to the same irrep as the ground state, the P space entering the CC(P)/EOMCC(P) calculations consists of all singly and doubly excited determinants and the subset of triply excited determinants captured by the CIPSI ground state. For the excited states belonging to other irreps, the P space defining the CC(P) problem is the same as that used for the ground state, but the lists of triples entering the EOMCC(P) diagonalizations are extracted from the CIPSI computations for the lowest-energy states of those other irreps.
3. Solve the CC(P) and, if excited states are targeted, EOMCC(P) equations in the P space or spaces obtained in Step 2. For the ground state and excited states belonging to the same irrep as the ground state, we define $T^{(P)} = T_1 + T_2 + T_3^{(\text{CIPSI})}$, $R_\mu^{(P)} = r_{\mu,0}\mathbf{1} + R_{\mu,1} + R_{\mu,2} + R_{\mu,3}^{(\text{CIPSI})}$, and $L_\mu^{(P)} = \delta_{\mu,0}\mathbf{1} + L_{\mu,1} + L_{\mu,2} + L_{\mu,3}^{(\text{CIPSI})}$, where the list of triples in $T_3^{(\text{CIPSI})}$, $R_{\mu,3}^{(\text{CIPSI})}$, and $L_{\mu,3}^{(\text{CIPSI})}$ is extracted from the CIPSI ground state. For the excited states belonging to other irreps, we construct the similarity-transformed Hamiltonian $\bar{H}^{(P)}$, to be diagonalized in the EOMCC(P) calculations, in the same way as in the ground-state computations, but $R_{\mu,3}^{(\text{CIPSI})}$ and $L_{\mu,3}^{(\text{CIPSI})}$ are defined using the lists of triples contained in the $|\Psi^{(\text{CIPSI})}\rangle$ wave functions that are the lowest-energy states of those irreps.
4. Determine corrections $\delta_\mu(P;Q)$, Eq. (4), describing the remaining T_3 and $R_{\mu,3}$ correlations not captured by the CIPSI-driven CC(P) and EOMCC(P) calculations, by defining the respective Q space(s) as those triply excited determinants that are outside the P space(s) considered in Steps 2 and 3. Add the resulting corrections $\delta_\mu(P;Q)$ to the CC(P)/EOMCC(P) energies $E_\mu^{(P)}$ to obtain the final CC($P;Q$) energies $E_\mu^{(P+Q)}$, Eq. (5).
5. To check convergence, repeat Steps 1–4 for some larger values of $N_{\text{det(in)}}$. The CIPSI-driven CC($P;Q$) calculations can be regarded as converged if the differences between consecutive $E_\mu^{(P+Q)}$ energies fall below a user-defined threshold. One can also consider stopping the calculations if the fraction(s) of triples contained in the final CIPSI state(s) $|\Psi^{(\text{CIPSI})}\rangle$ is (are) sufficiently large to produce the desired accuracy level with Eq. (5).

Similarly to the ground-state CIPSI-driven CC($P;Q$) approach of Refs. [31, 34], the above algorithm offers tremendous savings in computational effort relative to CCSDT/EOMCCSDT, which originate from three factors. First, as shown in the next section, the underlying CIPSI runs, needed to accurately approximate the parent CCSDT/EOMCCSDT energetics using the CC($P;Q$) method summarized above, rely on small $N_{\text{det(in)}}$ values resulting in compact CI spaces that are much smaller than the numbers of all triples employed in CCSDT/EOMCCSDT. Second, the CC(P) and EOMCC(P) calculations using tiny fractions of triples in the corresponding P spaces, such as those seen in the numerical examples discussed in this work, are one or more orders of magnitude faster than their CCSDT and EOMCCSDT counterparts. Third, the computational costs associated with the determination of the noniterative corrections $\delta_\mu(P;Q)$, which are similar – per state – to those characterizing the triples corrections of CCSD(T), CR-CC(2,3), or CR-EOMCC(2,3), are smaller than those of a single iteration of CCSDT/EOMCCSDT. The key elements of our algorithm used to implement the CC(P) equations, designed to efficiently handle small but generally spotty subsets of triply excited determinants identified by CIPSI, along with illustrative computational timings characterizing the ground-state CC($P;Q$) calculations, are described in the Appendix of Ref. [34]. We adopt a similar strategy when solving the EOMCC(P) equations. A detailed description of our efficient implementation of the CC(P) and EOMCC(P) equations and the CC($P;Q$) corrections targeting CCSDT/EOMCCSDT will be presented in a future publication.

3. Numerical examples

3.1. Computational details

To assess the ability of the excited-state extension of the CIPSI-driven CC($P;Q$) approach to converge EOMCCSDT energetics, we applied it to three molecular problems: (i) the frequently examined vertical excitations in the CH^+ ion, as described by the [5s3p1d/3s1p] basis set of Ref. [41], for which full EOMCCSDT is virtually exact [6, 7], that were used to test the semi-stochastic variant of CC($P;Q$) in Ref. [23], (ii) the adiabatic excitations in the CH radical, as described by the aug-cc-pVDZ basis [42, 43], used to test the semi-stochastic CC($P;Q$) method in Ref. [23] as well, which, in analogy to CH^+ , has low-lying excited states dominated by two-electron transitions requiring the EOMCCSDT theory level to obtain a reliable description [18, 44], and (iii) the ground- and excited-state

PESs of the water molecule, as described by the TZ basis set of Ref. [45], corresponding to the $\text{H}_2\text{O} \rightarrow \text{H} + \text{OH}$ dissociation, which, as demonstrated in Ref. [9], require the CCSDT/EOMCCSDT-level treatment to accurately approximate the full CI data and which were used to test the CC(t;3) and adaptive CC($P;Q$) algorithms in Ref. [9]. Our calculations for the CH^+ and CH systems were performed using the largest Abelian subgroup of $C_{\infty v}$, namely, C_{2v} . For the water molecule, where we were stretching one of the two O–H bonds, we used the relevant C_s symmetry. The CC(P)/EOMCC(P), CC($P;Q$) and CCSDT/EOMCCSDT computations for CH^+ and water relied on the RHF references, whereas the reference determinants used for CH were obtained using ROHF. Consistent with our prior semi-stochastic, adaptive, and active-orbital-based CC($P;Q$) studies of CH^+ , CH, and water [9, 23], in the post-ROHF calculations for CH and post-RHF computations for H_2O , the lowest core orbitals correlating with 1s shells of the carbon and oxygen atoms were frozen. In the case of CH^+ , we correlated all electrons. As in Refs. [31, 34], the CC(P), EOMCC(P), and CC($P;Q$) results discussed in the next three subsections, along with their CCSDT and EOMCCSDT parents, were obtained using our open-source CCPy package available on GitHub [46], which is interfaced with the RHF, ROHF, and integral-transformation routines in GAMESS [47], whereas the preceding CIPSI runs were executed with Quantum Package 2.0 [40]. In running CIPSI, we used the $N_{\text{det(in)}}$ values in the 1–20,000 range, so that the Hamiltonian diagonalization spaces generated by CIPSI were smaller than the numbers of triples used by CCSDT/EOMCCSDT, and we set the subspace enlargement factor f to its default value of 2 and the stopping parameter η to 10^{-6} hartree. With these choices of η and f , the CIPSI diagonalization sequences were terminated when the numbers of determinants in the $|\Psi^{(\text{CIPSI})}\rangle$ wave functions used to identify the subsets of triply excited determinants for inclusion in the P spaces adopted in our CC(P), EOMCC(P), and CC($P;Q$) calculations exceeded $N_{\text{det(in)}}$ and the $N_{\text{det(out)}}$ values characterizing the $|\Psi^{(\text{CIPSI})}\rangle$ states were always between $N_{\text{det(in)}}$ and $2N_{\text{det(in)}}$. The convergence threshold used in the CC(P)/EOMCC(P) and parent CCSDT/EOMCCSDT calculations was set to 10^{-7} hartree.

3.2. CH^+

Our first example is the CH^+ ion at the equilibrium ($R = R_e = 2.13713$ bohr; Table 1) and stretched ($R = 2R_e$; Table 2) geometries. For each C–H distance R , we examined vertical excitations corresponding to transitions from the ground state ($1^1\Sigma^+$) to the three lowest excited states of $1^1\Sigma^+$ symmetry, two lowest $1^1\Pi$ states, and two lowest $1^1\Delta$ states. In the case of the $n^1\Sigma^+$ ($n = 1$ –4) states, the lists of triples entering the three-body components of the $T^{(P)}$, $R_\mu^{(P)}$, and $L_\mu^{(P)}$ operators were extracted from the ground-state CIPSI runs initiated with the one-dimensional subspace $\mathcal{V}_{\text{int}}^{(0)}$ spanned by the RHF determinant. For the $n^1\Pi$ and $n^1\Delta$ ($n = 1, 2$) states, the three-body component of the cluster operator $T^{(P)}$, needed to construct the similarity-transformed Hamiltonian $\overline{H}^{(P)}$, was obtained in the same way as for the $1^1\Sigma^+$ states, but the lists of triples defining $R_{\mu,3}^{(\text{CIPSI})}$ and $L_{\mu,3}^{(\text{CIPSI})}$ in the subsequent EOMCC(P) diagonalizations were provided by the CIPSI runs targeting the lowest-energy states relevant to $1^1\Pi$ and $1^1\Delta$ symmetries, namely, the $1^1\text{B}_1(C_{2v})$ component of the $1^1\Pi$ state for the $n^1\Pi$ states and the $1^1\text{A}_2(C_{2v})$ component of the $1^1\Delta$ state for the $n^1\Delta$ states (initiated with the appropriate $3\sigma \rightarrow 1\pi$ and $3\sigma^2 \rightarrow 1\pi^2$ CSFs in the respective $\mathcal{V}_{\text{int}}^{(0)}$ subspaces).

To highlight the importance of enriching the P spaces used in the CC(P) and EOMCC(P) calculations with the leading triply excited determinants prior to evaluating the CC($P;Q$) corrections, we first discuss the results obtained using $N_{\text{det(in)}} = 1$, where the P spaces contain only singles and doubles. The EOMCC(P)/ $N_{\text{det(in)}} = 1$ approach is equivalent to EOMCCSD. Thus, it is not surprising that the EOMCC(P)/ $N_{\text{det(in)}} = 1$ results for the $2^1\Sigma^+$, $2^1\Pi$, $1^1\Delta$, and $2^1\Delta$ states at $R = R_e$ and for all seven excited states of CH^+ at $R = 2R_e$ considered in this study, which are dominated by two-electron transitions [6, 7] (with the $2^1\Delta$ state at $R = 2R_e$ also exhibiting substantial triple excitation character), are poor, producing errors relative to EOMCCSDT that are about 20, 12, 34, 35, and 14–144 millihartree, respectively. The EOMCC(P)/ $N_{\text{det(in)}} = 1$ calculations for the $3^1\Sigma^+$, $4^1\Sigma^+$, and $1^1\Pi$ states at $R = R_e$, which are dominated by single excitations, are more accurate, but the 3–6 millihartree errors relative to EOMCCSDT remain. The CC($P;Q$)/ $N_{\text{det(in)}} = 1$ corrections – equivalent to the triples corrections of CR-CC(2,3)/ CR-EOMCC(2,3) – are helpful, reducing the errors relative to EOMCCSDT in most cases to 1–3 millihartree, but they are ineffective for the $4^1\Sigma^+$ and $2^1\Delta$ states at $R = 2R_e$. For these two states, the energies obtained in the CC($P;Q$)/ $N_{\text{det(in)}} = 1$ calculations deviate from their EOMCCSDT counterparts by about 13 and 63 millihartree, respectively, which is telling us that to achieve an accurate description, the one- and two-body components of the cluster and EOM excitation and deexcitation operators must be relaxed in the presence of their three-body counterparts before evaluating the triples corrections. The CIPSI-driven CC($P;Q$) methodology enables this by increasing the $N_{\text{det(in)}}$ parameter and introducing the leading triply excited determinants into the P spaces employed in the CC(P) and EOMCC(P) computations.

Indeed, as shown in Tables 1 and 2, with as little as 1,178–1,792 $S_z = 0$ determinants of the $A_1(C_{2v})$, $B_1(C_{2v})$, and $A_2(C_{2v})$ symmetries in the terminal wave functions $|\Psi^{(\text{CIPSI})}\rangle$ corresponding to the lowest-energy $^1\Sigma^+$, $^1\Pi$, and $^1\Delta$ states of CH^+ generated by the inexpensive CIPSI runs using $N_{\text{det(in)}} = 1,000$, which capture tiny fractions, on the order of 0.7–3.7%, of the 31,912 $A_1(C_{2v})$ -symmetric, 27,180 $B_1(C_{2v})$ -symmetric, and 22,012 $A_2(C_{2v})$ -symmetric $S_z = 0$ triples used by CCSDT/EOMCCSDT, the differences between the energies of the $n^1\Sigma^+$ ($n = 2$ –4), $n^1\Pi$ ($n = 1, 2$), and $n^1\Delta$ ($n = 1, 2$) excited states of CH^+ at $R = R_e$ obtained with the CIPSI-driven CC($P;Q$) approach and their EOMCCSDT counterparts do not exceed 0.808 millihartree, being usually much smaller. At $R = 2R_e$, they do not exceed 1.282 millihartree, again being usually smaller. In particular, the large, 12.657 and 63.405 millihartree, errors relative to EOMCCSDT resulting from the $\text{CC}(P;Q)/N_{\text{det(in)}} = 1$ or CR-EOMCC(2,3) calculations for the $4^1\Sigma^+$ and $2^1\Delta$ states of CH^+ at $R = 2R_e$ reduce to less than 1 millihartree when the $\text{CC}(P;Q)/N_{\text{det(in)}} = 1,000$ method is employed. With the relatively small additional effort corresponding to $N_{\text{det(in)}} = 5,000$, which results in 5,392–9,446 $S_z = 0$ determinants of the $A_1(C_{2v})$, $B_1(C_{2v})$, and $A_2(C_{2v})$ symmetries in the final Hamiltonian diagonalization spaces adopted in the CIPSI-driven CC($P;Q$) runs, and only 5.7–16.8% of all triples in the underlying P spaces, the differences between the energies of the $n^1\Sigma^+$ ($n = 2$ –4), $n^1\Pi$ ($n = 1, 2$), and $n^1\Delta$ ($n = 1, 2$) excited states of CH^+ obtained in the CIPSI-driven CC($P;Q$) calculations and their EOMCCSDT parents reduce even further, to 0.005–0.207 millihartree at $R = R_e$ and 0.001–0.109 millihartree at $R = 2R_e$ (0.109 and 0.011 millihartree for the $4^1\Sigma^+$ and $2^1\Delta$ states at $R = 2R_e$). Clearly, these are substantial improvements compared to the CR-EOMCC(2,3) computations, which confirm the usefulness of incorporating the leading triply excited determinants identified by CIPSI in the CC(P) and EOMCC(P) calculations prior to the determination of the noniterative corrections $\delta_\mu(P;Q)$. Tables 1 and 2 also show that the previously observed [31, 34] acceleration in the convergence of the ground-state CC(P) energies toward their CCSDT parents offered by the CC($P;Q$) corrections applies to excited states and that the results of the CIPSI-driven CC($P;Q$) computations systematically improve when the fractions of triples captured by CIPSI increase.

3.3. CH

Our second example is the CH radical, where we examine energies of the ground and three lowest doublet excited states at their respective experimentally derived equilibrium geometries used in Refs. [18, 44] and our previous semi-stochastic CC($P;Q$) work [23], which are 1.1197868 Å for the $X^2\Pi$ ground state [48], 1.1031 Å for the $A^2\Delta$ state [48], 1.1640 Å for the $B^2\Sigma^-$ state [49], and 1.1143 Å for the $C^2\Sigma^+$ state [50] (Table 3). In analogy to CH^+ , the lists of triples defining the three-body components of the $T^{(P)}$, $R_\mu^{(P)}$, and $L_\mu^{(P)}$ operators adopted in the CIPSI-driven CC(P), EOMCC(P), and CC($P;Q$) calculations for CH were extracted from the terminal $|\Psi^{(\text{CIPSI})}\rangle$ wave functions representing the lowest-energy states of the relevant irreps of C_{2v} , *i.e.*, the $^2\text{B}_2(C_{2v})$ component of the $X^2\Pi$ state, the lowest state of $^2\text{A}_1(C_{2v})$ symmetry for the $A^2\Delta$ and $C^2\Sigma^+$ states, and the lowest $^2\text{A}_2(C_{2v})$ state for the $B^2\Sigma^-$ state. The $\mathcal{V}_{\text{int}}^{(0)}$ subspaces used to initiate the underlying CIPSI runs consisted of the $^2\text{B}_2(C_{2v})$ -symmetric ROHF determinant for the $X^2\Pi$ ground state, the $^2\text{A}_1(C_{2v})$ -symmetric determinant of the $3\sigma \rightarrow 1\pi$ type for the $A^2\Delta$ and $C^2\Sigma^+$ states, and the $3\sigma \rightarrow 1\pi/3\sigma 1\pi \rightarrow 1\pi^2$ CSF of the $^2\text{A}_2(C_{2v})$ symmetry for the $B^2\Sigma^-$ state.

As shown in Refs. [18, 44], all three excited states of CH examined here, especially $B^2\Sigma^-$ and $C^2\Sigma^+$ that are dominated by two-electron transitions, represent a significant challenge. This is manifested by the large errors relative to EOMCCSDT obtained for the $A^2\Delta$, $B^2\Sigma^-$, and $C^2\Sigma^+$ states with EOMCCSD (represented in Table 3 by $\text{EOMCC}(P)/N_{\text{det(in)}} = 1$), which are 13.474, 38.620, and 43.992 millihartree, respectively. The CR-EOMCC(2,3) triples corrections to EOMCCSD, equivalent to the $\text{CC}(P;Q)/N_{\text{det(in)}} = 1$ calculations, reduce these errors, being very effective for the $C^2\Sigma^+$ state, but the 7.727 millihartree error for the $A^2\Delta$ state and the 4.954 millihartree error for the $B^2\Sigma^-$ state remain. To address this situation, we turn to the CIPSI-driven CC($P;Q$) calculations with $N_{\text{det(in)}} > 1$. As shown in Table 3, already the inexpensive CC($P;Q$) computations using $N_{\text{det(in)}} = 1,000$, which rely on the compact CIPSI wave functions spanned by at most 1,889 $S_z = 1/2$ determinants that capture 1.0–3.9% of the 24,624–26,941 triples used by CCSDT/EOMCCSDT, reduce the 7.727 and 4.954 millihartree errors relative to EOMCCSDT for the $A^2\Delta$ and $B^2\Sigma^-$ states to 1.779 and 0.239 millihartree, respectively. Upon further increasing $N_{\text{det(in)}}$ to 5,000, which translates into terminal CIPSI diagonalization spaces that for the four states of CH listed in Table 3 are 3–4 times smaller than the numbers of triples used by CCSDT/EOMCCSDT and into 13.0–18.7% of all triples in the resulting P spaces, the CIPSI-driven CC($P;Q$) computations recover the parent CCSDT/EOMCCSDT energetics to within 0.051–0.367 millihartree, greatly improving the CR-CC(2,3)/CR-EOMCC(2,3) results for the $X^2\Pi$, $A^2\Delta$, and $B^2\Sigma^-$ states, while retaining high accuracy for the $C^2\Sigma^+$ state which CR-EOMCC(2,3) describes virtually perfectly. As in the case

of CH^+ , the CIPSI-driven $\text{CC}(P;Q)$ calculations accelerate convergence of the underlying $\text{CC}(P)/\text{EOMCC}(P)$ energetics toward $\text{CCSDT}/\text{EOMCCSDT}$ and become more accurate as the fractions of triples captured by CIPSI increase.

3.4. Potential cuts of H_2O

Finally, we examine the ground- and excited-state PES cuts of water along the $\text{H}_2\text{O} \rightarrow \text{H} + \text{OH}$ dissociation path constructed using 11 values of the O–H bond separation R_{OH} spanning 1.3 to 4.4 bohr and listed in Tables S1–S12 of the Supplementary Data document (Appendix A), with the remaining O–H bond length and $\angle\text{H–O–H}$ angle for each R_{OH} optimized using CCSD/cc-pVTZ in Ref. [45]. Following Ref. [8] and our recent active-orbital-based and adaptive $\text{CC}(P;Q)$ work [9], we considered the four lowest $\text{A}'(C_s)$ -symmetric singlet states (the $\text{X}^1\text{A}'$ ground state and the excited $n^1\text{A}'$ states with $n = 1–3$), the three lowest $\text{A}'(C_s)$ -symmetric triplet states ($n^3\text{A}'$, $n = 1–3$), the two lowest singlet states of the $\text{A}''(C_s)$ symmetry ($n^1\text{A}''$, $n = 1, 2$), and the three lowest $\text{A}''(C_s)$ -symmetric triplet states ($n^3\text{A}''$, $n = 1–3$). In analogy to CH^+ and CH , the lists of triples defining the $T_3^{(P)}$, $R_{\mu,3}^{(P)}$, and $L_{\mu,3}^{(P)}$ components of the $T^{(P)}$, $R_{\mu}^{(P)}$, and $L_{\mu}^{(P)}$ operators employed in the CIPSI-driven $\text{CC}(P)$, $\text{EOMCC}(P)$, and $\text{CC}(P;Q)$ calculations for H_2O were extracted from the terminal $|\Psi^{(\text{CIPSI})}\rangle$ wave functions corresponding to the lowest-energy states of the relevant symmetries, *i.e.*, we used the $S_z = 0$ triples of the $\text{A}'(C_s)$ symmetry for the $^1\text{A}'$ and $^3\text{A}'$ states and the $S_z = 0$ triples of the $\text{A}''(C_s)$ symmetry for the $^1\text{A}''$ and $^3\text{A}''$ states. The $\mathcal{V}_{\text{int}}^{(0)}$ subspaces used to initiate the underlying CIPSI runs consisted of the $\text{RHF} = |(1a')^2(2a')^2(3a')^2(4a')^2(1a'')^2|$ determinant for the A' states and the $1a'' \rightarrow 5a'$ CSFs for the A'' states. The results of our computations are reported in Tables 4 and 5, Fig. 1, and Supplementary Data. Tables 4 and 5 summarize the mean unsigned error (MUE) and nonparallelity error (NPE) values characterizing the PES cuts of water obtained in the CIPSI-driven $\text{CC}(P)/\text{EOMCC}(P)$ and $\text{CC}(P;Q)$ calculations relative to their nearly exact [9] $\text{CCSDT}/\text{EOMCCSDT}$ counterparts. Figure 1 shows the selected PES cuts associated with the $\text{H}_2\text{O} \rightarrow \text{H} + \text{OH}$ dissociation channels that correlate with the $\text{X}^2\Pi$ ground state and the lowest $^2\Sigma^+$ and $^2\Sigma^-$ states of the OH product. The total electronic energies for all the calculated states of water are provided in Supplementary Data.

In line with our earlier observations [8, 9], the CCSD/EOMCCSD and CR-CC(2,3)/CR-EOMCC(2,3) approaches, represented in Tables 4 and 5, Fig. 1, and Supplementary Data by the $N_{\text{det(in)}} = 1$ $\text{CC}(P)/\text{EOMCC}(P)$ and $\text{CC}(P;Q)$ computations, respectively, behave well near the equilibrium geometry on the ground-state PES. CR-CC(2,3) reduces the already small, 2.771–3.562 millihartree, errors in the CCSD energies relative to CCSDT for the $\text{X}^1\text{A}'$ ground state in the $R_{\text{OH}} = 1.3–2.0$ bohr region to 0.226–0.325 millihartree. For the excited states, the largest deviation from EOMCCSDT obtained in this region with EOMCCSD is 3.392 millihartree (for the $^3\text{A}'$ state). The largest error relative to EOMCCSDT produced in the same region by CR-EOMCC(2,3) is 1.660 millihartree (for the $^3\text{A}''$ state). With the exception of the $^3\text{A}''$, $^1\text{A}'$, and $^3\text{A}'$ states, the differences between the CR-EOMCC(2,3) and EOMCCSDT excited-state potentials in the $R_{\text{OH}} = 1.3–2.0$ bohr region are ~ 1 millihartree, confirming the utility of the CR-EOMCC(2,3) method in examining excited states of water in the vicinity of its equilibrium geometry [8]. The situation dramatically changes in the $R_{\text{OH}} > 2.0$ region, where nearly all electronic states of H_2O considered in this study acquire significant MR character, resulting in the large, 6.154–28.242 millihartree, MUEs and even larger, 8.453–64.664 millihartree, NPEs relative to CCSDT/EOMCCSDT obtained in the entire $R_{\text{OH}} = 1.3–4.4$ bohr region for the $\text{X}^1\text{A}'$, $^1\text{A}''$, $^1\text{A}''$, $^1\text{A}'$, $^2\text{A}'$, $^2\text{A}''$, $^2\text{A}'$, $^3\text{A}'$, $^3\text{A}'$, and $^3\text{A}'$ potentials with CCSD/EOMCCSD. The CR-CC(2,3)/CR-EOMCC(2,3) triples corrections to CCSD/EOMCCSD reduce the MUE and NPE values relative to CCSDT/EOMCCSDT for all 12 potential cuts of water examined in this work to 0.543–6.054 and 0.442–41.943 millihartree, respectively, but the substantial, 5.033 and 6.054 millihartree, MUEs and 13.044 and 41.943 millihartree NPEs obtained for the $^2\text{A}''$ and $^3\text{A}''$ states remain. The failure of CR-EOMCC(2,3) for the $^3\text{A}''$ state becomes particularly evident from the 36.791 millihartree error relative to EOMCCSDT at $R_{\text{OH}} = 2.8$ bohr, which results in a spurious bump in the $^3\text{A}''$ potential and the massive NPE of 41.943 millihartree [see Fig. 1(b) and Table 5].

To address the challenges encountered in the CR-EOMCC(2,3) calculations for some of the excited-state water potentials examined in this work, we again turn to the CIPSI-driven $\text{CC}(P;Q)$ approach with $N_{\text{det(in)}} > 1$. As shown in Tables 4 and 5 and Tables S1–S12 in Supplementary Data, already the $\text{CC}(P;Q)/N_{\text{det(in)}} = 1,000$ computations, which rely on the terminal $|\Psi^{(\text{CIPSI})}\rangle$ wave functions obtained in the inexpensive CIPSI runs that contain only 1,021–1,994 $S_z = 0$ determinants and 0.0–4.3% of the 31,832 $\text{A}'(C_s)$ -symmetric and 32,232 $\text{A}''(C_s)$ -symmetric $S_z = 0$ triples used by CCSDT/EOMCCSDT, provide substantial improvements, reducing the 0.543–6.054 millihartree MUEs and 0.442–41.943 millihartree NPEs relative to CCSDT/EOMCCSDT characterizing the CR-CC(2,3)/CR-EOMCC(2,3) potentials to 0.265–4.875 and 0.222–14.940 millihartree, respectively. With a modest increase in computational

effort corresponding to $N_{\text{det(in)}} = 5,000$, which results in 5,154–9,808 $S_z = 0$ determinants of the $A'(C_s)$ and $A''(C_s)$ symmetries in the final Hamiltonian diagonalization spaces adopted by CIPSI and only 3.1–15.9% of all triples in the respective P spaces, the CC($P;Q$) calculations produce further improvements, reproducing nearly all CCSDT/EOMCCSDT potentials considered in this study to within ~ 1 millihartree. The accuracy gains resulting from the CC($P;Q$)/ $N_{\text{det(in)}} = 5,000$ calculations are particularly impressive for the aforementioned $2^3A''$ and $3^3A''$ states that are poorly described by CR-EOMCC(2,3) (and even worse by the underlying EOMCCSD). In the case of the former state, the 5.033 millihartree MUE and 13.044 millihartree NPE relative to EOMCCSDT obtained with CR-EOMCC(2,3) reduce in the CC($P;Q$)/ $N_{\text{det(in)}} = 5,000$ computations to 0.695 and 0.559 millihartree, respectively. For the latter state, the CC($P;Q$)/ $N_{\text{det(in)}} = 5,000$ approach reduces the MUE and NPE values of 6.054 and 41.943 millihartree produced by CR-EOMCC(2,3) to 1.116 and 1.474 millihartree, respectively. In particular, the massive, 36.791 millihartree, error relative to EOMCCSDT obtained for the $3^3A''$ state at $R_{\text{OH}} = 2.8$ bohr with CR-EOMCC(2,3) is reduced in the CC($P;Q$)/ $N_{\text{det(in)}} = 5,000$ calculations to 1.680 millihartree, so that the unphysical bump on the CR-EOMCC(2,3) [or CC($P;Q$)/ $N_{\text{det(in)}} = 1$] PES of the $3^3A''$ state seen in the $R_{\text{OH}} \approx 2.8$ bohr region in Fig. 1(b) disappears [see Fig. 1(d)]. The results for the water molecule discussed here clearly demonstrate that the extension of our CIPSI-driven CC($P;Q$) methodology to excited states, as presented in this work, is very promising, allowing us to accurately approximate the EOMCCSDT energetics, even in challenging MR situations involving excited-state potentials along bond breaking coordinates, but there are two high-lying states in Tables 4 and 5, namely, $3^1A'$ and $3^3A'$, for which the convergence of the CIPSI-driven CC($P;Q$) energetics toward EOMCCSDT with $N_{\text{det(in)}}$ is slow (see, also, Tables S11 and S12 in Supplementary Data). This behavior arises because in our current implementation of the CIPSI-driven CC($P;Q$) approach aimed at CCSDT/EOMCCSDT, the underlying P spaces are tailored to the lowest-energy states of the relevant symmetries (in the case of the $3^1A'$ and $3^3A'$ states, the $S_z = 0$ determinants extracted from the CIPSI runs for the X^1A' ground state), which may be inadequate for describing higher-energy excited states, especially when the fractions of triples captured by CIPSI are small. We will return to this issue in future work by exploring state-specific P spaces extracted from excited-state CIPSI calculations.

4. Summary

We extended the CIPSI-driven CC($P;Q$) methodology of Refs. [31, 34] to excited states. The resulting approach, aimed at converging CCSDT/EOMCCSDT energetics, was tested on vertical excitations in CH^+ , adiabatic excitations in CH , and ground- and excited-state PES cuts of water along the O–H bond breaking coordinate. We demonstrated that for nearly all electronic states examined, it is sufficient to use small fractions of triply excited determinants in the underlying CC(P)/EOMCC(P) steps, identified by CIPSI runs involving relatively inexpensive Hamiltonian diagonalizations, to obtain CCSDT/EOMCCSDT-quality energetics, even when MR correlations and T_3 and $R_{\mu,3}$ effects are difficult to capture with the CR-CC(2,3)/CR-EOMCC(2,3) triples corrections to CCSD/EOMCCSD. Among our future plans are the exploration of state-specific variants of the CIPSI-driven CC($P;Q$) formalism, in which we will use CIPSI to design excitation spaces tailored to the electronic states of interest, and the pursuit of further reductions in computational costs by replacing the full CIPSI algorithm adopted in this work, which can explore the entire many-electron Hilbert space, with its truncated analogs (such as CIPSI truncated at triples or triples and quadruples).

CRediT authorship contribution statement

Swati S. Priyadarsini: Software, Data curation, Formal analysis, Investigation, Validation, Writing - original draft. **Karthik Gururangan:** Methodology, Software, Data curation, Formal analysis, Investigation, Validation, Writing - reviewing and editing. **Piotr Piecuch:** Conceptualization, Methodology, Formal analysis, Investigation, Funding acquisition, Project administration, Resources, Supervision, Validation, Writing - reviewing and editing.

Declaration of competing interest

The authors declare that they have no known competing financial interests or personal relationships that could have appeared to influence the work reported in this paper.

Data availability

The data that support the findings of this study are available within the article and the Supplementary Data.

Acknowledgments

This work has been supported by the Chemical Sciences, Geosciences and Biosciences Division, Office of Basic Energy Sciences, Office of Science, U.S. Department of Energy (Grant No. DE-FG02-01ER15228 to P.P.).

Appendix A. Supplementary data

Supplementary material associated with this article can be found online at

References

- [1] J. F. Stanton, R. J. Bartlett, The equation of motion coupled-cluster method. A systematic biorthogonal approach to molecular excitation energies, transition probabilities, and excited state properties, *J. Chem. Phys.* 98 (1993) 7029–7039. doi:10.1063/1.464746.
- [2] J. Čížek, On the correlation problem in atomic and molecular systems. Calculation of wavefunction components in Ursell-type expansion using quantum-field theoretical methods, *J. Chem. Phys.* 45 (1966) 4256–4266. doi:10.1063/1.1727484.
- [3] J. Paldus, J. Čížek, I. Shavitt, Correlation problems in atomic and molecular systems. IV. Extended coupled-pair many-electron theory and its application to the BH_3 molecule, *Phys. Rev. A* 5 (1972) 50–67. doi:10.1103/PhysRevA.5.50.
- [4] H. J. Monkhorst, Calculation of properties with the coupled-cluster method, *Int. J. Quantum Chem., Symp.* 11 (1977) 421–432. doi:10.1002/qua.560120850.
- [5] H. Nakatsuji, Cluster expansion of the wavefunction. Excited states, *Chem. Phys. Lett.* 59 (1978) 362–364. doi:10.1016/0009-2614(78)89113-1.
- [6] K. Kowalski, P. Piecuch, The active-space equation-of-motion coupled-cluster methods for excited electronic states: Full EOMCCSDt, *J. Chem. Phys.* 115 (2001) 643–651. doi:10.1063/1.1378323.
- [7] K. Kowalski, P. Piecuch, Excited-state potential energy curves of CH^+ : A comparison of the EOMCCSDt and full EOMCCSDt results, *Chem. Phys. Lett.* 347 (2001) 237–246. doi:10.1016/S0009-2614(01)01010-7.
- [8] J. J. Lutz, P. Piecuch, Performance of the completely renormalized equation-of-motion coupled-cluster method in calculations of excited-state potential cuts of water, *Comput. Theor. Chem.* 1040–1041 (2014) 20–34. doi:10.1016/j.comptc.2014.05.008.
- [9] K. Gururangan, J. Shen, P. Piecuch, Extension of the active-orbital-based and adaptive $\text{CC}(P;Q)$ approaches to excited electronic states: Application to potential cuts of water, *Chem. Phys. Lett.* 862 (2025) 141840. doi:<https://doi.org/10.1016/j.cplett.2024.141840>.
- [10] P. Piecuch, J. A. Hansen, A. O. Ajala, Benchmarking the completely renormalised equation-of-motion coupled-cluster approaches for vertical excitation energies, *Mol. Phys.* 113 (2015) 3085–3127. doi:10.1080/00268976.2015.1076901.
- [11] S. A. Kucharski, M. Włoch, M. Musiał, R. J. Bartlett, Coupled-cluster theory for excited electronic states: The full equation-of-motion coupled-cluster single, double, and triple excitation method, *J. Chem. Phys.* 115 (2001) 8263–8266. doi:10.1063/1.1416173.

[12] J. D. Watts, R. J. Bartlett, Economical triple excitation equation-of-motion coupled-cluster methods for excitation energies, *Chem. Phys. Lett.* 233 (1995) 81–87. doi:10.1016/0009-2614(94)01434-W.

[13] O. Christiansen, H. Koch, P. Jørgensen, Perturbative triple excitation corrections to coupled cluster singles and doubles excitation energies, *J. Chem. Phys.* 105 (1996) 1451–1459. doi:10.1063/1.472007.

[14] J. D. Watts, R. J. Bartlett, Iterative and non-iterative triple excitation corrections in coupled-cluster methods for excited electronic states: The EOM-CCSDT-3 and EOM-CCSD(T) methods, *Chem. Phys. Lett.* 258 (1996) 581–588. doi:10.1016/0009-2614(96)00708-7.

[15] O. Christiansen, H. Koch, P. Jørgensen, Response functions in the CC3 iterative triple excitation model, *J. Chem. Phys.* 103 (1995) 7429–7441. doi:10.1063/1.470315.

[16] K. Kowalski, P. Piecuch, New coupled-cluster methods with singles, doubles, and noniterative triples for high accuracy calculations of excited electronic states, *J. Chem. Phys.* 120 (2004) 1715–1738. doi:10.1063/1.1632474.

[17] M. Włoch, M. D. Lodriguito, P. Piecuch, J. R. Gour, Two new classes of non-iterative coupled-cluster methods derived from the method of moments of coupled-cluster equations, *Mol. Phys.* 104 (2006) 2149–2172, 104 (2006) 2991 [Erratum]. doi:10.1080/00268970600659586.

[18] P. Piecuch, J. R. Gour, M. Włoch, Left-eigenstate completely renormalized equation-of-motion coupled-cluster methods: Review of key concepts, extension to excited states of open-shell systems, and comparison with electron-attached and ionized approaches, *Int. J. Quantum Chem.* 109 (2009) 3268–3304. doi:10.1002/qua.22367.

[19] G. Fradelos, J. J. Lutz, T. A. Wesołowski, P. Piecuch, M. Włoch, Embedding vs supermolecular strategies in evaluating the hydrogen-bonding-induced shifts of excitation energies, *J. Chem. Theory Comput.* 7 (2011) 1647–1666. doi:10.1021/ct200101x.

[20] J. Shen, P. Piecuch, Biorthogonal moment expansions in coupled-cluster theory: Review of key concepts and merging the renormalized and active-space coupled-cluster methods, *Chem. Phys.* 401 (2012) 180–202. doi:10.1016/j.chemphys.2011.11.033.

[21] S. Hirata, M. Nooijen, I. Grabowski, R. J. Bartlett, Perturbative corrections to coupled-cluster and equation-of-motion coupled-cluster energies: A determinantal analysis, *J. Chem. Phys.* 114 (2001) 3919–3928, 115 (2001) 3967–3968 [Erratum]. doi:10.1063/1.1346578.

[22] T. Shiozaki, K. Hirao, S. Hirata, Second- and third-order triples and quadruples corrections to coupled-cluster singles and doubles in the ground and excited states, *J. Chem. Phys.* 126 (2007) 244106. doi:10.1063/1.2741262.

[23] S. H. Yuwono, A. Chakraborty, J. E. Deustua, J. Shen, P. Piecuch, Accelerating convergence of equation-of-motion coupled-cluster computations using the semi-stochastic CC($P;Q$) formalism, *Mol. Phys.* 118 (2020) e1817592. doi:10.1080/00268976.2020.1817592.

[24] J. Shen, P. Piecuch, Combining active-space coupled-cluster methods with moment energy corrections via the CC($P;Q$) methodology, with benchmark calculations for biradical transition states, *J. Chem. Phys.* 136 (2012) 144104. doi:10.1063/1.3700802.

[25] J. Shen, P. Piecuch, Merging active-space and renormalized coupled-cluster methods via the CC($P;Q$) formalism, with benchmark calculations for singlet-triplet gaps in biradical systems, *J. Chem. Theory Comput.* 8 (2012) 4968–4988. doi:10.1021/ct300762m.

[26] N. P. Bauman, J. Shen, P. Piecuch, Combining active-space coupled-cluster approaches with moment energy corrections via the CC($P;Q$) methodology: Connected quadruple excitations, *Mol. Phys.* 115 (2017) 2860–2891. doi:10.1080/00268976.2017.1350291.

[27] I. Magoulas, N. P. Bauman, J. Shen, P. Piecuch, Application of the CC($P;Q$) hierarchy of coupled-cluster methods to the beryllium dimer, *J. Phys. Chem. A* 122 (2018) 1350–1368. doi:10.1021/acs.jpca.7b10892.

[28] S. H. Yuwono, I. Magoulas, J. Shen, P. Piecuch, Application of the coupled-cluster CC($P;Q$) approaches to the magnesium dimer, *Mol. Phys.* 117 (2019) 1486–1506. doi:10.1080/00268976.2018.1564847.

[29] J. E. Deustua, J. Shen, P. Piecuch, Converging high-level coupled-cluster energetics by Monte Carlo sampling and moment expansions, *Phys. Rev. Lett.* 119 (2017) 223003. doi:10.1103/PhysRevLett.119.223003.

[30] J. E. Deustua, J. Shen, P. Piecuch, High-level coupled-cluster energetics by Monte Carlo sampling and moment expansions: Further details and comparisons, *J. Chem. Phys.* 154 (2021) 124103. doi:10.1063/5.0045468.

[31] K. Gururangan, J. E. Deustua, J. Shen, P. Piecuch, High-level coupled-cluster energetics by merging moment expansions with selected configuration interaction, *J. Chem. Phys.* 155 (2021) 174114. doi:10.1063/5.0064400.

[32] A. Chakraborty, S. H. Yuwono, J. E. Deustua, J. Shen, P. Piecuch, Benchmarking the semi-stochastic CC($P;Q$) approach for singlet–triplet gaps in biradicals, *J. Chem. Phys.* 157 (2022) 134101. doi:10.1063/5.0100165.

[33] K. Gururangan, P. Piecuch, Converging high-level coupled-cluster energetics via adaptive selection of excitation manifolds driven by moment expansions, *J. Chem. Phys.* 159 (2023) 084108. doi:10.1063/5.0162873.

[34] S. S. Priyadarsini, K. Gururangan, J. Shen, P. Piecuch, The singlet–triplet gap of cyclobutadiene: The CIPSI-driven CC($P;Q$) study, *J. Phys. Chem. A* 129 (2025) 11749–11780. doi:<https://doi.org/10.1021/acs.jpca.5c07572>.

[35] P. Piecuch, M. Włoch, Renormalized coupled-cluster methods exploiting left eigenstates of the similarity-transformed Hamiltonian, *J. Chem. Phys.* 123 (2005) 224105. doi:10.1063/1.2137318.

[36] J. Noga, R. J. Bartlett, The full CCSDT model for molecular electronic structure, *J. Chem. Phys.* 86 (1987) 7041–7050, 89 (1988) 3401 [Erratum]. doi:10.1063/1.452353.

[37] G. E. Scuseria, H. F. Schaefer, III, A new implementation of the full CCSDT model for molecular electronic structure, *Chem. Phys. Lett.* 152 (1988) 382–386. doi:10.1016/0009-2614(88)80110-6.

[38] B. Huron, J. P. Malrieu, P. Rancurel, Iterative perturbation calculations of ground and excited state energies from multiconfigurational zeroth-order wavefunctions, *J. Chem. Phys.* 58 (1973) 5745–5759. doi:<https://doi.org/10.1063/1.1679199>.

[39] Y. Garniron, A. Scemama, P.-F. Loos, M. Caffarel, Hybrid stochastic-deterministic calculation of the second-order perturbative contribution of multireference perturbation theory, *J. Chem. Phys.* 147 (2017) 034101. doi:<https://doi.org/10.1063/1.4992127>.

[40] Y. Garniron, T. Applencourt, K. Gasperich, A. Benali, A. Ferté, J. Paquier, B. Pradines, R. Assaraf, P. Reinhardt, J. Toulouse, P. Barbaresco, N. Renon, G. David, J.-P. Malrieu, M. Véril, M. Caffarel, P.-F. Loos, E. Giner, A. Scemama, Quantum Package 2.0: An open-source determinant-driven suite of programs, *J. Chem. Theory Comput.* 15 (2019) 3591–3609. doi:<https://doi.org/10.1021/acs.jctc.9b00176>.

[41] J. Olsen, A. M. Sánchez de Merás, H. J. A. Jensen, P. Jørgensen, Excitation energies, transition moments and dynamic polarizabilities for CH⁺. A comparison of multiconfigurational linear response and full configuration interaction calculations, *Chem. Phys. Lett.* 154 (1989) 380–386. doi:10.1016/0009-2614(89)85373-4.

[42] T. H. Dunning, Jr., Gaussian basis sets for use in correlated molecular calculations. I. The atoms boron through neon and hydrogen, *J. Chem. Phys.* 90 (1989) 1007–1023. doi:10.1063/1.456153.

[43] R. A. Kendall, T. H. Dunning, Jr., R. J. Harrison, Electron affinities of the first-row atoms revisited. Systematic basis sets and wave functions, *J. Chem. Phys.* 96 (1992) 6796–6806. doi:10.1063/1.462569.

[44] S. Hirata, Higher-order equation-of-motion coupled-cluster methods, *J. Chem. Phys.* 121 (2004) 51–59. doi: 10.1063/1.1753556.

[45] X. Li, J. Paldus, Performance of multireference and equation-of-motion coupled-cluster methods for potential energy surfaces of low-lying excited states: Symmetric and asymmetric dissociation of water, *J. Chem. Phys.* 133 (2010) 024102. doi:10.1063/1.3451074.

[46] K. Gururangan, J. E. Deustua, and P. Piecuch, “CCPy: A Coupled-Cluster Package Written in Python,” see <https://github.com/piecuch-group/ccpy> [software].

[47] G. M. J. Barca, C. Bertoni, L. Carrington, D. Datta, N. De Silva, J. E. Deustua, D. G. Fedorov, J. R. Gour, A. O. Gunina, E. Guidez, T. Harville, S. Irle, J. Ivanic, K. Kowalski, S. S. Leang, H. Li, W. Li, J. J. Lutz, I. Magoulas, J. Mato, V. Mironov, H. Nakata, B. Q. Pham, P. Piecuch, D. Poole, S. R. Pruitt, A. P. Rendell, L. B. Roskop, K. Ruedenberg, T. Sattasathuchana, M. W. Schmidt, J. Shen, L. Slipchenko, M. Sosonkina, V. Sundriyal, A. Tiwari, J. L. G. Vallejo, B. Westheimer, M. Włoch, P. Xu, F. Zahariev, M. S. Gordon, Recent developments in the general atomic and molecular electronic structure system, *J. Chem. Phys.* 152 (2020) 154102. doi: 10.1063/5.0005188.

[48] M. Zachwieja, New investigations of the $A^2\Delta - X^2\Pi$ band system in the CH radical and a new reduction of the vibration-rotation spectrum of CH from the ATMOS spectra, *J. Mol. Spectrosc.* 170 (1995) 285–309. doi:10.1006/jmsp.1995.1072.

[49] R. Kępa, A. Para, M. Rytel, M. Zachwieja, New spectroscopic analysis of the $B^2\Sigma^- - X^2\Pi$ band system of the CH molecule, *J. Mol. Spectrosc.* 178 (1996) 189–193. doi:10.1006/jmsp.1996.0173.

[50] K. P. Huber, G. Herzberg, *Molecular Spectra and Molecular Structure: IV. Constants of Diatomic Molecules*, Van Nostrand Reinhold, New York, 1979. doi:10.1007/978-1-4757-0961-2.

Table 1

Convergence of the CIPSI-based CC(P)/EOMCC(P) and CC($P;Q$) energies toward CCSDT/EOMCCSDT for the CH^+ ion, as described by the [5s3p1d/3s1p] basis set of Ref. [41], at the C–H internuclear distance $R = R_e = 2.13713$ bohr. The P spaces used in the CC(P) and EOMCC(P) calculations were defined as all singly and doubly excited determinants and subsets of triply excited determinants extracted from the terminal $|\Psi(\text{CIPSI})\rangle$ wave functions obtained in the CIPSI runs for the lowest-energy states of the relevant symmetries, as described in the main text (see, also, footnote ‘a’). The Q spaces used to construct the CC($P;Q$) corrections $\delta_\mu(P;Q)$ consisted of the remaining triples not captured by CIPSI.

$N_{\text{det}(\text{in})}$	$1^1\Sigma^+$			$2^1\Sigma^+$			$3^1\Sigma^+$			$4^1\Sigma^+$			$1^1\Pi$			$2^1\Pi$			$1^1\Delta$			$2^1\Delta$		
	$N_{\text{det}(\text{out})}$	$\%T^{\text{b}}$	P^{c}	$(P;Q)^{\text{d}}$																				
1 ^e	1	0.0	1.845	0.063	19.694	1.373	3.856	0.787	5.536	0.954	2	0.0	3.080	0.792	11.636	2.805	2	0.0	34.304	-0.499	34.685	0.350		
1,000	1,347	0.7	0.932	0.021	12.386	0.808	3.127	0.599	2.902	0.112	1,286	2.9	0.769	0.189	3.825	0.545	1,178	2.6	2.084	0.181	10.072	0.467		
5,000	5,392	5.7	0.171	0.005	4.117	0.207	0.325	0.066	0.479	0.061	6.610	13.9	0.138	0.044	2.041	0.154	9.446	16.8	0.087	0.023	1.082	0.066		
10,000	10,798	11.6	0.062	0.001	0.889	0.062	-0.039	0.043	0.256	0.032	13.226	23.3	0.043	0.020	1.190	0.042	19.156	26.9	0.026	0.009	0.317	0.018		
20,000	21,602	21.4	0.019	0.000	0.201	0.015	-0.115	0.019	0.161	0.013	23.756	34.0	0.018	0.009	0.181	0.012	32.778	36.7	0.010	0.004	0.179	0.006		

^a For each value of $N_{\text{det}(\text{in})}$, $N_{\text{det}(\text{out})}$ is the total number of determinants in the corresponding terminal $|\Psi(\text{CIPSI})\rangle$ wave function obtained in a CIPSI run for the lowest state of a given symmetry [the $1^1\Sigma^+ = 1^1\text{A}_1(C_{2v})$ ground state for the Σ^+ states, the $1^1\text{B}_1(C_{2v})$ component of the $1^1\Pi$ states, and the $1^1\text{A}_2(C_{2v})$ component of the $1^1\Delta$ state for the $1^1\Delta$ states].

^b The $\%T$ values are the percentages of triply excited determinants contained in the terminal CIPSI wave functions $|\Psi(\text{CIPSI})\rangle$ described in footnote ‘a’.

^c Errors in the CC(P) (the $1^1\Sigma^+$ ground state) and EOMCC(P) (excited states) energies, in millihartree, relative to the CCSDT and EOMCCSDT data. The CCSDT energy for the $1^1\Sigma^+$ state is -38.019516 hartree. The EOMCCSDT energies for the $2^1\Sigma^+$, $3^1\Sigma^+$, $4^1\Sigma^+$, $1^1\Pi$, $2^1\Pi$, $1^1\Delta$, and $2^1\Delta$ states are -37.702621 , -37.522457 , -37.386872 , -37.900921 , -37.498143 , -37.762113 , and -37.402308 hartree, respectively.

^d Errors, in millihartree, in the CC($P;Q$) energies relative to the corresponding CCSDT and EOMCCSDT data provided in footnote ‘c’.

^e The CC(P) and EOMCC(P) energies at $N_{\text{det}(\text{in})} = 1$ are identical to the energies obtained in the CCSD and EOMCCSD calculations. The corresponding CC($P;Q$) energies are equivalent to the CR-CC(2,3) (the ground state) and CR-EOMCC(2,3) (excited state) results.

Table 2
Same as Table 1 for the stretched C–H internuclear distance $R = 2R_e = 4.27426$ bohr.^a

$N_{\text{det(in)}}$	$1^1\Sigma^+$			$2^1\Sigma^+$			$3^1\Sigma^+$			$4^1\Sigma^+$			$1^1\Pi$			$2^1\Pi$			$1^1\Delta$			$2^1\Delta$			
	$N_{\text{det(out)}}$	%T	P	($P;Q$)	P	($P;Q$)	P	($P;Q$)	$N_{\text{det(out)}}$	%T	P	($P;Q$)	$N_{\text{det(out)}}$	%T	P	($P;Q$)	$N_{\text{det(out)}}$	%T	P	($P;Q$)	$N_{\text{det(out)}}$	%T	P	($P;Q$)	
1	1	0.0	5,002	0.012	17,140	1,646	19,929	-2,870	32,639	12,657	2	0.0	13,552	2,303	21,200	-1,428	2	0.0	44,495	-4,525	144,414	-63,405			
1,000	1,677	1.8	0.434	0.005	7,457	1,096	10,848	-1,282	9,609	0.999	1,792	3.2	0.452	0.046	1,758	0.095	1,764	3.7	0.430	0.046	8,160	0.855			
5,000	6,719	7.7	0.060	0.001	0.852	0.034	0.889	0.011	1,860	0.109	7,180	11.0	0.052	0.006	0.159	0.012	6,962	10.8	0.047	0.008	0.408	0.011			
10,000	13,163	15.3	0.016	0.000	0.404	0.010	0.446	0.008	0.760	0.055	14,362	19.2	0.013	0.002	0.043	0.003	13,312	17.4	0.015	0.004	0.144	0.002			
20,000	24,508	24.7	0.003	0.000	0.098	0.005	0.096	0.005	0.148	0.007	27,560	29.6	0.003	0.001	0.015	0.003	28,274	28.1	0.004	0.002	0.037	0.000			

^a The CCSDT energy for the $1^1\Sigma^+$ state is -37.900394 hartree. The EOMCCSDT energies for the $2^1\Sigma^+$, $3^1\Sigma^+$, $4^1\Sigma^+$, $1^1\Pi$, $2^1\Pi$, $1^1\Delta$, and $2^1\Delta$ states are -37.704834 , -37.650242 , -37.495275 , -37.879532 , -37.702345 , -37.714180 , and -37.494031 hartree, respectively.

Table 3

Convergence of the CIPSI-based CC(P)/EOMCC(P) and CC($P;Q$)/EOMCCSDT for the CH radical, as described by the aug-cc-pVDZ basis set [42, 43]. The P spaces used in the CC(P) and EOMCC(P) calculations were defined as all singly and doubly excited determinants and subsets of triply excited determinants extracted from the terminal $|\Psi^{(\text{CIPSI})}\rangle$ wave functions obtained in the CIPSI runs for the lowest-energy states of the relevant symmetries, as described in the main text (see, also, footnote ‘a’). The Q spaces used to construct the CC($P;Q$) corrections $\delta_\mu(P;Q)$ consisted of the remaining triples not captured by CIPSI.

$N_{\text{det}(\text{in})}$	X $^2\Pi$				A $^2\Delta$				B $^2\Sigma^-$				C $^2\Sigma^+$			
	$N_{\text{det}(\text{out})}$ ^a	%T ^b	P^c	($P;Q$) ^d	$N_{\text{det}(\text{out})}$ ^a	%T ^b	P^c	($P;Q$) ^d	$N_{\text{det}(\text{out})}$ ^a	%T ^b	P^c	($P;Q$) ^d	$N_{\text{det}(\text{out})}$ ^a	%T ^b	P^c	($P;Q$) ^d
1 ^e	1	0.0	2.987	0.231	1	0.0	13.474	7.727	3	0.0	38.620	-4.954	1	0.0	43.992	0.087
1,000	1,154	1.0	2.909	0.227	1,677	3.3	6.482	1.779	1,790	3.9	5.914	0.239	1,889	3.9	10.044	0.922
5,000	9,247	16.4	0.917	0.051	6,586	13.0	1.410	0.266	7,184	18.7	2.167	0.367	7,567	14.7	1.747	0.309
10,000	18,501	34.0	0.418	0.019	13,425	24.4	0.585	0.115	14,373	34.6	1.172	0.204	11,014	20.3	1.310	0.209
20,000	37,016	62.5	0.096	0.003	26,851	43.4	0.190	0.034	28,755	54.9	0.569	0.080	22,870	38.5	0.690	0.091

^a For each value of $N_{\text{det}(\text{in})}$, $N_{\text{det}(\text{out})}$ is the total number of determinants in the corresponding terminal $|\Psi^{(\text{CIPSI})}\rangle$ wave function obtained in a CIPSI run for the lowest state of a given symmetry [the $^2\text{B}_2(\text{C}_{2v})$ component of the $\text{X}^2\Pi$ ground state, the lowest $^2\text{A}_1(\text{C}_{2v})$ state for the $\text{A}^2\Delta$ and $\text{C}^2\Sigma^+$ states, and the lowest $^2\text{A}_2(\text{C}_{2v})$ state for the $\text{B}^2\Sigma^-$ state].

^b The %T values are the percentages of triply excited determinants contained in the terminal CIPSI wave functions $\Psi^{(\text{CIPSI})}$ described in footnote ‘a’.

^c Errors in the CC(P) (the $\text{X}^2\Pi$ ground state) and EOMCC(P) (excited states) energies, in millihartree, relative to the CCSDT and EOMCCSDT data, calculated at the experimentally derived equilibrium C–H bond lengths used in Refs. [18, 44], which are 1.1197868 Å for the $\text{X}^2\Pi$ state [48], 1.1031 Å for the $\text{A}^2\Delta$ state [48], 1.1640 Å for the $\text{B}^2\Sigma^-$ state [49], and 1.1143 Å for the $\text{C}^2\Sigma^+$ state [50]. The CCSDT and EOMCCSDT energies for the $\text{X}^2\Pi$, $\text{A}^2\Delta$, $\text{B}^2\Sigma^-$, and $\text{C}^2\Sigma^+$ states at these geometries are -38.387749, -38.276770, -38.267544, and -38.238205 hartree, respectively.

^d Errors, in millihartree, in the CC($P;Q$) energies relative to the corresponding CCSDT and EOMCCSDT data, obtained at the experimentally derived equilibrium C–H bond lengths used in Refs. [18, 44] and listed in footnote ‘c’.

^e The CC(P) and EOMCC(P) energies at $N_{\text{det}(\text{in})} = 1$ are identical to the energies obtained in the CCSD and EOMCCSD calculations. The corresponding CC($P;Q$) energies are equivalent to the CR-CC(2,3) (ground state) and CR-EOMCC(2,3) (excited states) results.

Table 4

The MUE values, in millihartree, relative to CCSDT/EOMCCSDT characterizing the ground- and 11 excited-state potential cuts of the water molecule, as described by the TZ basis set of Ref. [45], along the O–H bond-breaking coordinate corresponding to the $\text{H}_2\text{O} \rightarrow \text{H} + \text{OH}$ dissociation obtained with the CIPSI-based $\text{CC}(P)/\text{EOMCC}(P)$ and $\text{CC}(P;Q)$ approaches examined in the present work. The P spaces used in the $\text{CC}(P)$ and $\text{EOMCC}(P)$ calculations were defined as all singly and doubly excited determinants and subsets of triply excited determinants extracted from the terminal $|\Psi^{(\text{CIPSI})}\rangle$ wave functions obtained in the CIPSI runs for the lowest-energy states of the relevant symmetries, as described in the main text (see, also, footnote ‘b’). The Q spaces used to construct the $\text{CC}(P;Q)$ corrections $\delta_\mu(P;Q)$ consisted of the remaining triples not captured by CIPSI.

State	$N_{\text{det(in)}} = 1^{\text{a}}$		$N_{\text{det(in)}} = 1,000$		$N_{\text{det(in)}} = 5,000$		$N_{\text{det(in)}} = 10,000$		$N_{\text{det(in)}} = 20,000$	
	%T=0.0 ^b		%T=0.0–4.3 ^b		%T=3.1–15.9 ^b		%T=8.1–23.7 ^b		%T=16.7–34.7 ^b	
	P^{c}	$(P;Q)^{\text{d}}$	P^{c}	$(P;Q)^{\text{d}}$	P^{c}	$(P;Q)^{\text{d}}$	P^{c}	$(P;Q)^{\text{d}}$	P^{c}	$(P;Q)^{\text{d}}$
$\text{X}^1\text{A}'$	6.154	0.543	3.342	0.265	1.453	0.068	0.884	0.031	0.411	0.011
$1^1\text{A}''$	7.666	1.517	2.941	0.853	1.240	0.660	0.805	0.458	0.449	0.249
$1^3\text{A}'$	2.819	1.137	2.361	1.111	1.057	0.504	1.060	0.380	0.531	0.176
$1^3\text{A}''$	7.693	1.080	3.164	0.908	1.318	0.666	0.863	0.449	0.484	0.237
$1^1\text{A}'$	10.103	1.544	9.599	0.728	7.050	0.514	5.184	0.381	3.460	0.169
$2^3\text{A}'$	8.846	1.225	8.413	0.744	6.311	0.479	4.326	0.304	3.121	0.128
$2^3\text{A}''$	9.258	5.033	8.440	2.549	4.174	0.695	3.092	0.376	1.574	0.199
$2^1\text{A}'$	14.460	2.988	9.019	0.764	3.984	0.580	3.066	0.423	1.652	0.284
$2^1\text{A}''$	2.337	1.750	5.108	1.652	3.626	0.586	3.096	0.315	1.631	0.174
$3^3\text{A}''$	28.242	6.054	18.471	4.875	6.634	1.116	3.917	0.544	1.850	0.250
$3^1\text{A}'$	13.467	2.329	11.648	2.715	7.022	2.388	5.452	2.003	4.087	1.672
$3^3\text{A}'$	8.305	2.481	6.899	2.622	4.712	1.358	3.379	1.051	2.324	0.826

^a The MUE values characterizing the $\text{CC}(P)$ and $\text{EOMCC}(P)$ calculations at $N_{\text{det(in)}} = 1$ are identical to those obtained with CCSD and EOMCCSD. The corresponding $\text{CC}(P;Q)$ MUEs are equivalent to those obtained with CR-CC(2,3) (the ground state) and CR-EOMCC(2,3) (excited states).

^b The %T for a given $N_{\text{det(in)}}$ is the percentage ($N_{\text{det(in)}} = 1$) or the range of percentages ($N_{\text{det(in)}} = 1,000$ –20,000) of the $S_z = 0$ triply excited determinants captured by the CIPSI runs for the lowest-energy states of the relevant symmetries [$\text{X}^1\text{A}'(C_s)$ for the $^1\text{A}'$ and $^3\text{A}'$ states and $1^1\text{A}''(C_s)$ for the $^1\text{A}''$ and $^3\text{A}''$ states] at the various geometries of H_2O used to construct the ground- and excited-state potentials considered in the present study.

^c The MUE values characterizing the ground-state $\text{CC}(P)$ and excited-state $\text{EOMCC}(P)$ potentials relative to their CCSDT and EOMCCSDT parents.

^d The MUE values characterizing the ground- and excited-state $\text{CC}(P;Q)$ potentials relative to their CCSDT and EOMCCSDT parents.

Table 5

The NPE values, in millihartree, relative to CCSDT/EOMCCSDT characterizing the ground- and 11 excited-state potential cuts of the water molecule, as described by the TZ basis set of Ref. [45], along the O–H bond-breaking coordinate corresponding to the $\text{H}_2\text{O} \rightarrow \text{H} + \text{OH}$ dissociation obtained with the CIPSI-based $\text{CC}(P)/\text{EOMCC}(P)$ and $\text{CC}(P;Q)$ approaches examined in the present work. The P spaces used in the $\text{CC}(P)$ and $\text{EOMCC}(P)$ calculations were defined as all singly and doubly excited determinants and subsets of triply excited determinants extracted from the terminal $|\Psi^{(\text{CIPSI})}\rangle$ wave functions obtained in the CIPSI runs for the lowest-energy states of the relevant symmetries, as described in the main text (see, also, footnote ‘b’). The Q spaces used to construct the $\text{CC}(P;Q)$ corrections $\delta_\mu(P;Q)$ consisted of the remaining triples not captured by CIPSI.

State	$N_{\text{det}(\text{in})} = 1^{\text{a}}$		$N_{\text{det}(\text{in})} = 1,000$		$N_{\text{det}(\text{in})} = 5,000$		$N_{\text{det}(\text{in})} = 10,000$		$N_{\text{det}(\text{in})} = 20,000$	
	%T=0.0 ^b		%T=0.0–4.3 ^b		%T=3.1–15.9 ^b		%T=8.1–23.7 ^b		%T=16.7–34.7 ^b	
	P^{c}	$(P;Q)^{\text{d}}$	P^{c}	$(P;Q)^{\text{d}}$	P^{c}	$(P;Q)^{\text{d}}$	P^{c}	$(P;Q)^{\text{d}}$	P^{c}	$(P;Q)^{\text{d}}$
$\text{X}^1\text{A}'$	8.453	0.692	1.744	0.222	1.191	0.075	0.644	0.035	0.396	0.015
$1^1\text{A}''$	16.093	4.592	4.532	0.556	1.967	0.322	1.705	0.241	1.478	0.214
$1^3\text{A}'$	5.004	0.442	4.431	0.617	2.279	0.375	3.161	0.264	2.078	0.155
$1^3\text{A}''$	17.445	3.303	4.967	0.532	2.377	0.336	2.135	0.221	1.792	0.224
$1^1\text{A}'$	21.043	4.637	21.133	0.502	17.668	0.789	11.340	0.513	8.503	0.487
$2^3\text{A}'$	20.127	3.712	19.157	0.530	17.008	0.678	9.436	0.463	8.207	0.399
$2^3\text{A}''$	29.017	13.044	24.403	4.875	7.586	0.559	4.900	0.421	2.587	0.213
$2^1\text{A}'$	33.260	8.330	33.344	2.574	10.982	0.659	9.262	0.536	4.990	0.643
$2^1\text{A}''$	7.971	3.983	14.093	2.814	5.408	0.389	4.300	0.405	2.844	0.280
$3^3\text{A}''$	64.664	41.943	47.469	14.940	9.412	1.474	6.643	0.541	2.744	0.262
$3^1\text{A}'$	30.847	4.376	30.966	5.012	15.483	5.282	10.661	5.198	9.084	5.065
$3^3\text{A}'$	21.562	5.670	16.356	6.617	14.339	2.605	8.617	2.461	7.195	2.411

^a The NPE values characterizing the $\text{CC}(P)$ and $\text{EOMCC}(P)$ calculations at $N_{\text{det}(\text{in})} = 1$ are identical to those obtained with CCSD and EOMCCSD. The corresponding $\text{CC}(P;Q)$ NPEs are equivalent to those obtained with CR-CC(2,3) (the ground state) and CR-EOMCC(2,3) (excited states).

^b The %T for a given $N_{\text{det}(\text{in})}$ is the percentage ($N_{\text{det}(\text{in})} = 1$) or the range of percentages ($N_{\text{det}(\text{in})} = 1,000$ –20,000) of the $S_z = 0$ triply excited determinants captured by the CIPSI runs for the lowest-energy states of the relevant symmetries [$\text{X}^1\text{A}'(C_s)$ for the $^1\text{A}'$ and $^3\text{A}'$ states and $1^1\text{A}''(C_s)$ for the $^1\text{A}''$ and $^3\text{A}''$ states] at the various geometries of H_2O used to construct the ground- and excited-state potentials considered in the present study.

^c The NPE values characterizing the ground-state $\text{CC}(P)$ and excited-state $\text{EOMCC}(P)$ potentials relative to their CCSDT and EOMCCSDT parents.

^d The NPE values characterizing the ground- and excited-state $\text{CC}(P;Q)$ potentials relative to their CCSDT and EOMCCSDT parents.

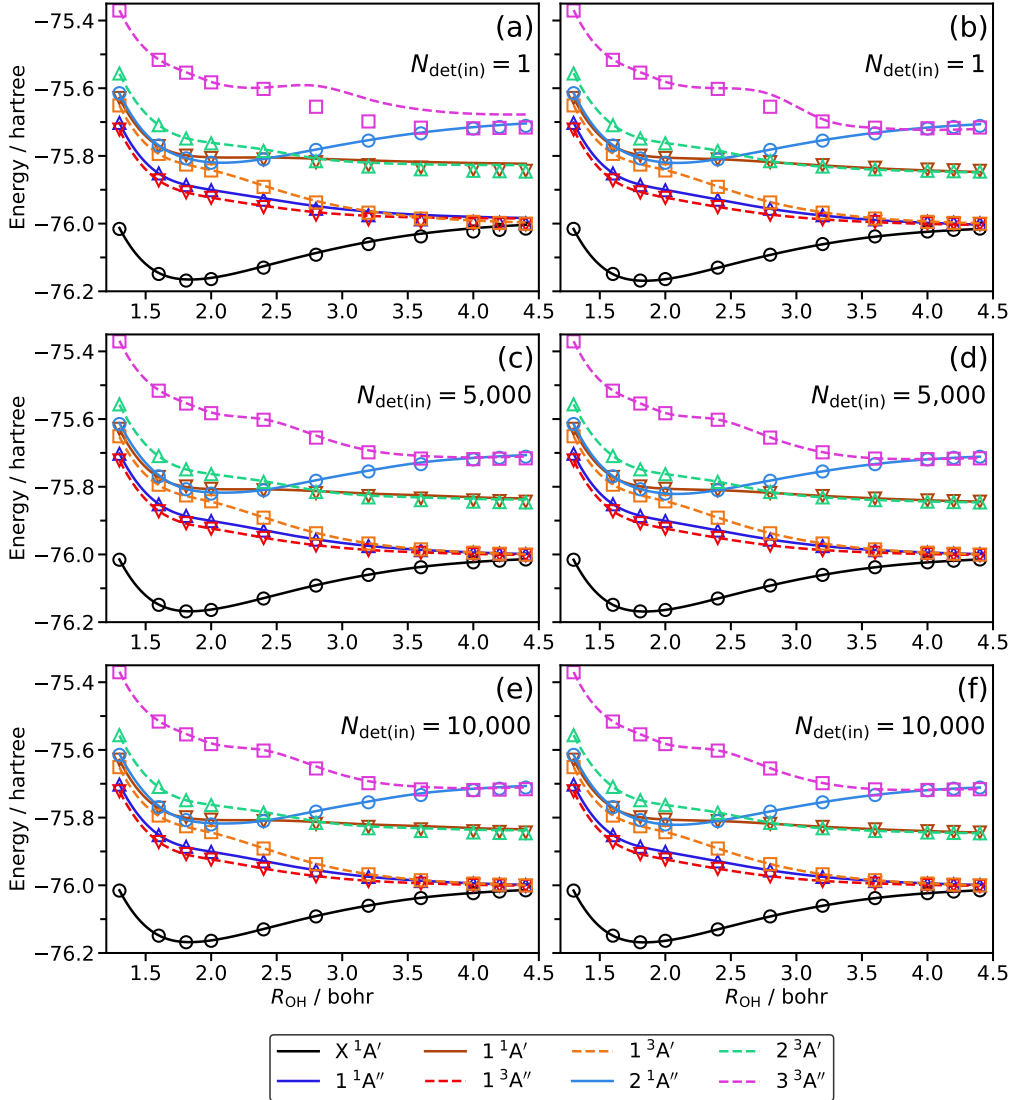


Fig. 1. A comparison of the PES cuts of water along the O–H bond breaking coordinate R_{OH} for the $\text{H}_2\text{O} \rightarrow \text{H} + \text{OH}$ dissociation channels correlating with the $\text{X}^2\Pi$ ground state and the lowest-energy $^2\Sigma^+$ and $^2\Sigma^-$ states of the OH product resulting from the CIPSI-driven CC(P)/EOMCC(P) [panels (a), (c), and (e)] and CC($P;Q$) [panels (b), (d), and (f)] calculations at selected values of the CIPSI wave function termination parameter $N_{\text{det}(\text{in})}$ with their full CCSDT/EOMCCSDT counterparts. The solid and dashed lines represent the splined CC(P)/EOMCC(P) and CC($P;Q$) data, whereas the open circles, squares, triangles, and inverted triangles denote the parent CCSDT/EOMCCSDT energetics. The CC(P)/EOMCC(P) and CC($P;Q$) results shown in panels (a) and (b), obtained with $N_{\text{det}(\text{in})} = 1$, are equivalent to the CCSD/EOMCCSD and CR-CC(2,3)/CR-EOMCC(2,3) calculations, respectively.